Fluorescence Turn-on Responses of Anionic and Cationic Conjugated Polymers toward Proteins: Effect of Electrostatic and Hydrophobic Interactions

Kan-Yi Pu and Bin Liu*

Department of Chemical and Biomolecular Engineering, 4 Engineering Drive 4, National University of Singapore, Singapore 117576

Received: July 8, 2009; Revised Manuscript Received: November 25, 2009

Cationic and anionic poly(fluorenyleneethynylene-*alt*-benzothiadiazole)s (PFEBTs) are designed and synthesized *via* Sonagashira coupling reaction to show light-up signatures toward proteins. Due to the charge transfer character of the excited states, the fluorescence of PFEBTs is very weak in aqueous solution, while their yellow fluorescence can be enhanced by polymer aggregation. PFEBTs show fluorescence turn-on rather than fluorescence quenching upon complexation with proteins. Both electrostatic and hydrophobic interactions between PFEBTs and proteins are found to improve the polymer fluorescence, the extent of which is dependent on the nature of the polymer and the protein. Changes in solution pH adjust the net charges of proteins, providing an effective way to manipulate electrostatic interactions and in turn the increment in the polymer fluorescence. In addition, the effect of protein digestion on the fluorescence of polymer/protein complexes is probed. The results indicate that electrostatic interaction induced polymer fluorescence increase cannot be substantially reduced through cleaving protein into peptide fragments. In contrast, hydrophobic interactions, mainly determined by the hydrophobicity of proteins, can be minimized by digestion, imparting a light-off signature for the polymer/protein complexes. This study thus not only highlights the opportunities of exerting nonspecific interactions for protein sensing but also reveals significant implications for biosensor design.

Introduction

Research in genomics and proteomics has stimulated the pursuit of novel technologies for efficient, convenient, and precise detection of biomolecules.[1] Since many diseases do not have a specific genetic signature but rather a variation in protein expression, biosensors for protein detection are of particular significance in medical diagnostics and pathogen recognition.[2] Proteins are much more complex and sensitive than oligonucleotides, which require additional severe considerations in the course of assay design.[3] A crucial challenge for the development of protein biosensors consists in the design of materials featuring appropriate receptors for efficient binding with the target protein, simultaneously coupled with the control of structure and functionality for competent signal transduction. Conjugated polyelectrolytes (CPEs), integrating the electrostatic behaviors of polyelectrolytes with the optoelectronic properties of π-conjugated polymers, provide an excellent platform for the construction of protein biosensors.[4] Their electron-delocalized backbones facilitate rapid intrachain and interchain exciton migrations *via* fluorescence resonance energy transfer (FRET), resulting in amplified signals and improved sensitivity relative to small fluorophores.[5] Therefore, CPE-based assays hold great promise in high throughput screening of proteins.

CPE-based protein assays involving "lock-key" recognition have been reported.[6] For instance, cationic polythiophene (PT) in conjunction with a nucleic acid ligand (aptamer) was utilized to detect human thrombin based on the conformation-dependent colorimetric behaviors of PT.[6c,d] Recently, we took advantage of dye-labeled aptamer/protein specific binding and light-harvesting properties of CPEs to enable FRET-based lysozyme detection in biological media.[7] The participation of FRET realized a dual-channel signal collection and thereby further enhanced detection selectivity. In these assays, specific aptamer/protein binding cooperates with nonspecific CPE/biomolecule interactions to generate optical responses. The signal-to-noise ratio is reported to be affected by nonspecific interactions between CPEs and disturbing proteins.[8]

On the contrary, nonspecific interaction induced perturbation in photophysical properties of CPEs has been exploited for protein detection. Fluorescence quenching of CPEs in the presence of proteins *via* electron transfer or aggregation mechanisms allowed protein discrimination according to the pattern of Stern−Volmer quenching constants,[9] and a protein sensor array has been built with six water-soluble poly(*p*-phenylene ethynylene)s (PPEs).[10] Recently, we synthesized a series of anionic polyfluorene (PF) derivatives comprising different fractions of 2,1,3-benzothiadiazole (BT) units for multicolor protein sensing. The polymer aggregation driven by nonspecific interactions led to solution fluorescent color changes dependent on the different nature of each protein.[11]

In spite of the preliminary success in using nonspecific interactions for protein detection, the underlying mechanisms of how electrostatic and hydrophobic interactions between CPEs and proteins would individually influence the photophysical properties of CPEs and in turn affect protein sensing are poorly understood. Previous investigations revealed that electrostatic attractions between CPEs and charged small molecules led to polymer aggregation and in turn fluorescence self-quenching.[11] In contrast, hydrophobic interactions between CPEs and nonionic amphiphilic surfactant could impel a hydrophobic environment, giving rise to increased polymer fluorescence.[12] However, electrostatic and hydrophobic interactions usually coexist in CPE/protein systems to induce a *countercurrent*-mixed optical response for most CPEs,[13] making the analysis of the effect of CPE/protein interactions on the polymer fluorescence compli-

* To whom correspondence should be addressed. E-mail: cheliub@nus.edu.sg.

10.1021/jp906433u
Published on Web 01/29/2010

SCHEME 1: Synthesis of PFEBT$^-$ and PFEBT$^+$ [a]

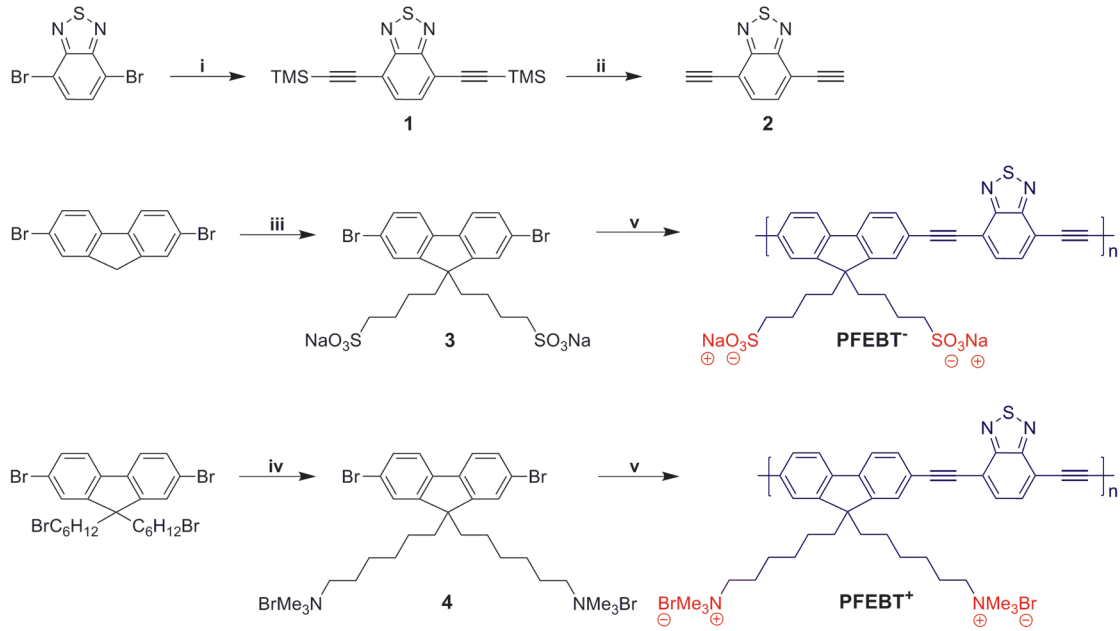

[a] Reagents and conditions: (i) trimethylsilyl acetylene, $Pd(PPh_3)_4$/CuI, $(iPr)_2NH$/THF, 70 °C, 12 h; (ii) KOH aqueous solution, THF/CH_3OH, 0 °C, 3 h; (iii) 1,4-butane sultone, TBAB, DMSO/NaOH aqueous solution, room temperature; (iv) NMe_3, THF/H_2O, 24 h; (v) **2**, $Pd(PPh_3)_4$/CuI, DMF/H_2O/$(i$Pr$)_2$NH, 70 °C, 24 h.

cated or even impossible. As such, to overcome this problem, CPEs with the *concurrent* optical response toward both electrostatic and hydrophobic interactions are desirable.

Water-soluble BT-containing polyfluorene derivatives are efficient multicolor probes for detection and quantification of biomoleucles, including DNA,[14] heparin,[15] and proteins.[11] Recently, we found that BT fluorescence was sensitive to the environmental polarity owing to the charge transfer character of the polymer's excited states.[16] The weak polymer fluorescence in aqueous solution was enhanced by polymer aggregation which provided a hydrophobic refuge for the polymer against water invasion. Considering that both electrostatic and hydrophobic interactions can induce polymer aggregation, the environment-sensitive fluorescence of BT-based CPEs is appropriate for analysis of the effect of CPE/protein interactions on the polymer fluorescence.

In this contribution, we report two new light-up macromolecules, cationic and anionic poly(fluorenyleneethynylene-*alt*-benzothiadiazole)s (PFEBTs), and utilize them to reveal the roles of electrostatic and hydrophobic interactions in the fluorescence response of CPEs toward proteins. We first describe the synthesis and intrinsic optical properties of PFEBTs, which is followed by examining their fluorescence turn-on responses toward bovine serum albumin (BSA) and lysozyme in buffer at pH 7.4. BSA and lysozyme are chosen to interact with PFEBTs in view of their opposite net charges over a wide pH range. To illustrate the role of electrostatic interactions in the polymer fluorescence, the solution pH is adjusted to tune the net charges of proteins. Finally, the fluorescence variations of PFEBTs upon protein digestion by pepsin are investigated to probe the contribution of hydrophobic interactions to the protein-induced fluorescence response of PFEBTs.

Results and Discussion

Synthesis and Characterization. The synthetic route toward poly[9,9-bis(4′-sulfonatobutyl)fluorenyleneethynylene-*alt*-4,7-(2,1,3,-benzothiadiazole) disodium] (PFEBT$^-$) and poly[9,9-bis(6′-(*N*,*N*,*N*,-trimethylammonium)-hexyl)fluorenyleneethynylene-*alt*-4,7-(2,1,3,-benzothiadiazole) dibromide] (PFEBT$^+$) is depicted in Scheme 1. The starting materials, 4,7-dibromobenzothiadiazole and 2,7-dibromo-9,9-bis(6′-bromohexyl)fluorene, were synthesized according to our previous report.[17] 4,7-Bis(2-(trimethylsilyl)ethynyl)benzothiadiazole (**1**) was prepared *via* a $Pd(PPh_3)_4$/CuI catalyzed Sonagashira coupling reaction between 4,7-dibromobenzothiadiazole and trimethylsilyl acetylene.[18] Due to the lower reactivity of 4,7-dibromobenzothiadiazole as compared to its diiodide counterpart, $Pd(PPh_3)_4$ instead of $(Ph_3P)_2PdCl_2$ was used as the catalyst in this reaction.[19] The diyne monomer 4,7-diethynylbenzothiadiazole (**2**) was obtained after deprotecting the trimethylsilyl groups of **1** in a basic solution. 2,7-Dibromo-9,9-bis(4′-sulfonatobutyl)fluorene disodium (**3**) was synthesized in 60% yield by reacting 2,7-dibromofluorene with 1,4-butane sultone in a mixture of aqueous NaOH (50 wt %) and dimethyl sulfoxide (DMSO) in the presence of tetrabutylammonium bromide (TBAB).[20] Quaternization of 9,9-bis(6′-bromohexyl)fluorene with trimethylamine in THF/H_2O afforded 2,7-dibromo-9,9-bis(6′-(*N*,*N*,*N*,-trimethylammonium)-hexyl)fluorene dibromide (**4**) in a high yield (98%). The correct chemical structures of **1**, **3**, and **4** were affirmed by NMR and mass spectra. The water-soluble dibromide monomers **3** and **4** were respectively polymerized with **2** *via* the $Pd(PPh_3)_4$/CuI catalyzed Sonagashira coupling polymerization in a mixed solvent of DMF/H_2O/diisopropylamine (2:1:1.5) to directly give the water-soluble polymers PFEBT$^-$ and PFEBT$^+$. These polymers were purified by precipitation, microfiltration, and finally dialysis against Mill-Q water using a 3.5 kDa molecular weight cutoff dialysis membrane for 5 days. The chemical structures of PFEBT$^-$ and PFEBT$^+$ were characterized by NMR spectra.

Optical Properties. The UV−vis absorption and photoluminescence (PL) spectra of PFEBT$^-$ and PFEBT$^+$ in water are shown in Figure 1. The polymer concentration based on repeating unit (RU) is 2 μM. The spectral profiles for PFEBT$^-$ and PFEBT$^+$ are similar. In the absorption spectra, two bands

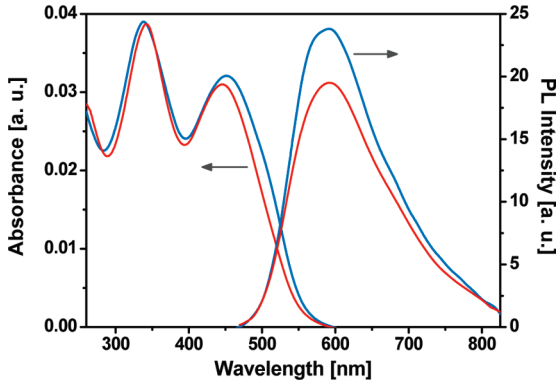

Figure 1. UV−vis absorption and PL spectra of $PFEBT^-$ (red) and $PFEBT^+$ (blue) in water. [RU] = 2 μM, excitation at 445 nm.

centered at 339 and 450 nm are observed for both polymers, which correspond to the fluorenyleneethynylene units and the BT units, respectively. In the PL spectra, both $PFEBT^-$ and $PFEBT^+$ show an emission maximum at ~598 nm. The PL quantum yields of $PFEBT^-$ and $PFEBT^+$ in water are ~0.009 and 0.011, respectively, measured using quinine sulfate in 0.1 M H_2SO_4 (quantum yield = 0.55) as the reference. However, the PL quantum yields of $PFEBT^-$ and $PFEBT^+$ in methanol are 0.07 and 0.10, respectively, which are much higher than those in water. Calculations on the electronic structure of neutral poly(fluorene-*alt*-BT) (PFBT) revealed that the lowest unoccupied molecular orbital (LUMO) is preferentially localized on the BT units and there is charge redistribution upon excitation of the polymer due to the strong electron deficiency of the BT units.[21] These predicted optical properties of neutral PFBT have been experimentally witnessed, as shown in our recent report.[16] PFEBTs, with similar backbone structures to PFBT, thus should also have the charge-transfer electronic states. This is reflected by the solvent polarity dependent quantum yields and the large Stokes shift (148 nm) of PFEBTs in water. As such, aggregation-enhanced fluorescent behaviors in aqueous solution are anticipated for PFEBTs.

Light-Up Response toward Protein. The fluorescence responses of PFEBTs toward BSA and lysozyme are investigated in 15 mM PBS at pH 7.4. Figure 2a and b shows the PL spectra of $PFEBT^-$ and $PFEBT^+$ at [RU] = 6 μM in the presence of BSA with [BSA] ranging from 0 to 0.8 μM at intervals of 0.1 μM upon excitation at 445 nm. Both $PFEBT^-$ and $PFEBT^+$ exhibit fluorescence enhancement upon BSA addition. Moreover, the emission maxima for both polymers are blue-shifted from ~598 nm in the absence of BSA to ~588 nm in the presence of 0.8 μM BSA. It has been widely reported that BSA, a fatty acid transporter with surfactant effect, often leads to increased fluorescence and blue-shifted emission maxima for chromophores.[22] The similar spectral variations of PFEBTs upon BSA addition are thus due to the increased hydrophobicity of the polymer environment that reduces the contact between the water molecules and the electron-delocalized conjugated backbone.

The PL intensities at 588 nm for $PFEBT^-$ and $PFEBT^+$ at [RU] = 6 μM as a function of [BSA] are compared in Figure 2c. Although $PFEBT^-$ and $PFEBT^+$ have nearly similar PL intensities in the absence of BSA, the PL intensity for $PFEBT^+$ at each [BSA] is much higher than that for $PFEBT^-$. The largest difference in the PL intensity is observed at [BSA] = 0.8 μM where the fluorescence response toward BSA saturates for both polymers. At this point, the PL intensities for $PFEBT^-$ and $PFEBT^+$ are 153 and 466 au, which are 5.7- and 17.3-fold of

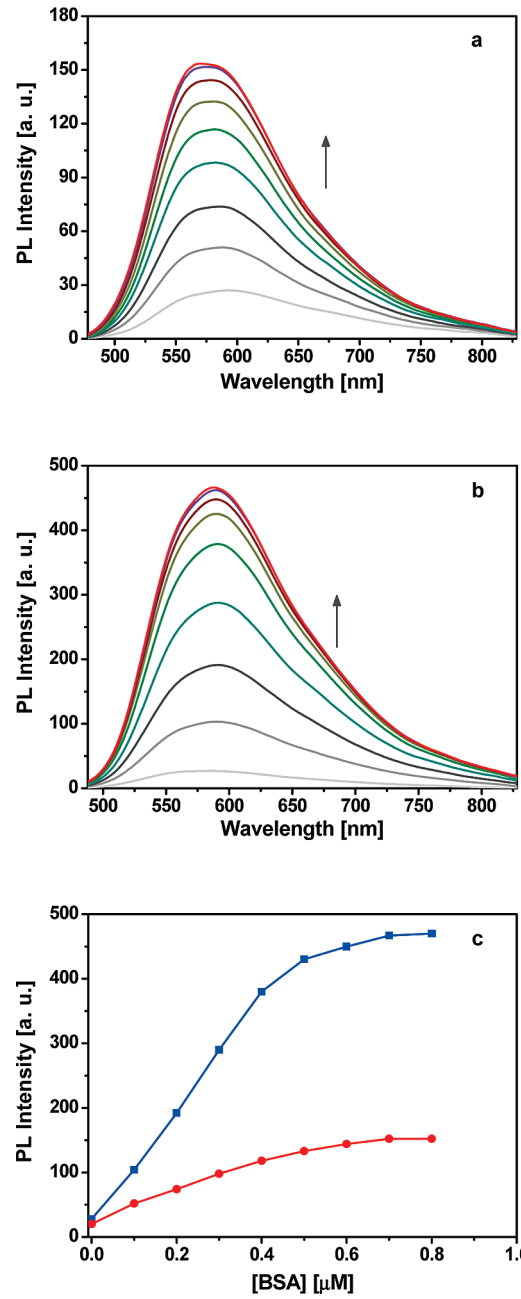

Figure 2. PL spectra of (a) $PFEBT^-$ and (b) $PFEBT^+$ in the presence of BSA with [BSA] ranging from 0 to 0.8 μM at intervals of 0.1 μM. The arrows indicate increasing [BSA]. (c) PL intensities at 588 nm for $PFEBT^+$ (blue squares) and $PFEBT^-$ (red circles) as a function of [BSA]. [RU] = 6 μM in 15 mM PBS at pH 7.4, excitation at 445 nm.

those in the absence of BSA, respectively. Since the isoelectric point (pI) value of BSA is ~4.8, at pH 7.4, BSA has net negative charges. Accordingly, strong electrostatic attractions apart from hydrophobic interactions occur between oppositely charged $PFEBT^+$ and BSA at pH 7.4, while hydrophobic interactions should be the main driving force for the molecular interaction between $PFEBT^-$ and BSA. Due to the discrepancy in the polymer/protein interactions, the complexes for $PFEBT^+$/BSA have shown higher fluorescence intensities than that for $PFEBT^-$/BSA.

The PL spectra of $PFEBT^-$ and $PFEBT^+$ at [RU] = 6 μM in the absence and presence of lysozyme are also monitored. As shown in Figure 3a, with increasing [lysozyme], the PL intensity of $PFEBT^-$ gradually increases until [lysozyme] reaches 0.8

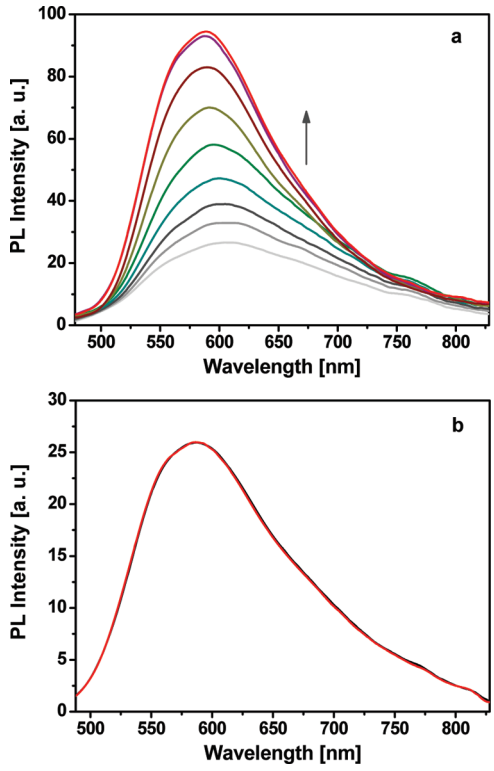

Figure 3. (a) PL spectra of PFEBT$^-$ in the presence of lysozyme with [lysozyme] ranging from 0 to 0.8 μM at intervals of 0.1 μM. The arrow indicates increasing [lysozyme]. (b) PL spectra of PFEBT$^+$ in the absence of lysozyme and in the presence of 0.8 μM lysozyme. [RU] = 6 μM in 15 mM PBS at pH 7.4, excitation at 445 nm.

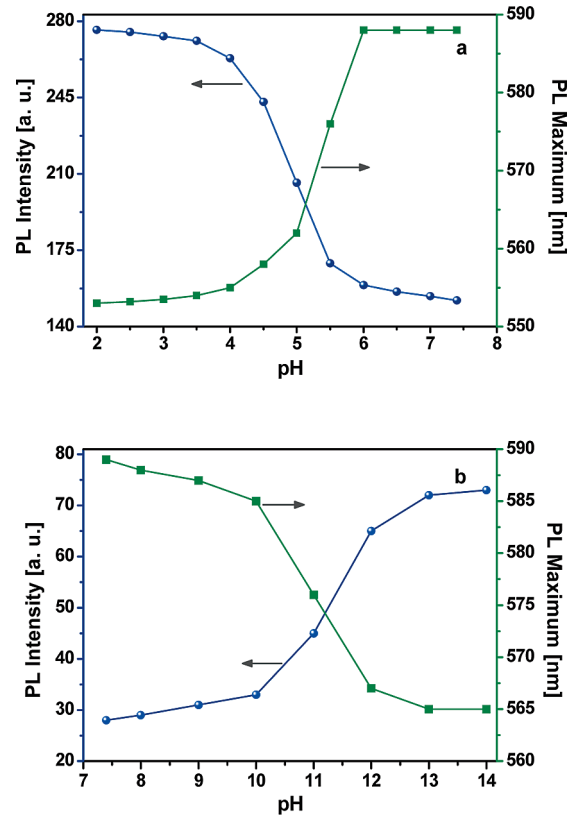

Figure 4. PL maxima (λ_{max}) and PL intensities at λ_{max} for (a) PFEBT$^-$/BSA and (b) PFEBT$^+$/lysozyme as a function of pH. [RU] = 6 μM and [protein] = 0.8 μM in 15 mM buffer, excitation at 445 nm.

μM. At the saturation point, the PL intensity of PFEBT$^-$ is 94 au, which is ~3.6-fold more intense than that in the absence of lysozyme. This phenomenon is opposite to the previous reports where lysozyme/CPE interaction induced polymer fluorescence quenching.[8] The PL spectra of PFEBT$^+$ in the absence of lysozyme and in the presence of 0.8 μM lysozyme are presented in Figure 3b. No spectral variation is observed for PFEBT$^+$ upon lysozyme addition. According to the pI of lysozyme (~11), lysozyme has net positive charges at pH 7.4. Strong electrostatic attractions occur between oppositely charged PFEBT$^-$ and lysozyme, leading to polymer aggregation and thereby the enhanced fluorescence. On the contrary, electrostatic repulsions exist between PFEBT$^+$ and lysozyme. Lysozyme (13.930 kDa), which is much smaller and less amphiphilic than BSA (69.323 kDa), does not have remarkable surfactant-like properties.[23] As such, PFEBT$^+$ exhibits no fluorescence response toward lysozyme at pH 7.4.

Effect of pH on Fluorescence of Polymer/Protein Complex. On account of the pH-variable net charges of proteins, the effect of pH on the fluorescence of polymer/protein complexes is examined to investigate the role of electrostatic attractions in the fluorescence turn-on response of PFEBTs. It should be noted that both PFEBT$^-$ and PFEBT$^+$ do not show obvious fluorescence change with pH varying from 2 to 14. Since PFEBT$^-$/BSA and PFEBT$^+$/lysozyme have weak electrostatic attractions at pH 7.4 as aforementioned, they were chosen as the polymer/protein pairs for pH effect study.

The PL experiments were conducted in 15 mM buffer at [RU] = 6 μM and [protein] = 0.8 μM. These concentrations are identical to those at saturation points shown in Figures 2 and 3a. Figure 4a summarizes the changes in the fluorescence of PFEBT$^-$/BSA as a function of pH ranging from 7.4 to 2 upon excitation at 445 nm. With decreasing pH, the PL maximum (λ_{max}) of PFEBT$^-$/BSA is blue-shifted, and the PL intensity at λ_{max} increases. In addition, obvious transformations for the PL maximum and intensity curves occur in the pH range from 6 to 4. At pH 2, the PL maximum of PFEBT$^-$/BSA is 556 nm, which is blue-shifted by 32 nm as compared to that at pH 7.4 (588 nm); its intensity also increases from 151 au at pH 7.4 to 273 au at pH 2. Similar phenomena happen to PFEBT$^+$/lysozyme complexes. Figure 4b depicts the changes in the fluorescence of PFEBT$^+$/lysozyme as a function of pH ranging from 7.4 to 14 upon excitation at 445 nm. With increasing pH, light-up response of PFEBT$^+$ toward lysozyme appears. The PL maximum (λ_{max}) of PFEBT$^+$/lysozyme is blue-shifted from 588 nm at pH 7.4 to 565 nm at pH 14, while the PL intensity increases from 28 au at pH 7.4 to 73 au at pH 14. In addition, a large transformation for the PL spectra is observed in the pH range from 10 to 12.

These data show that the fluorescence of PFEBT/protein complexes can be effectively manipulated by pH, due to the pH-dependent change in protein net charges.[24] As reported previously, the net charges of BSA at pH 7.4 and 4.5 are around −17 and +29, respectively,[25] and the net charges of lysozyme at pH 7.4 and 12 are around +8 and −3, respectively.[26] Accordingly, decreasing the pH from 7.4 to 2 gradually reverses the net charge of BSA from negative to positive, resulting in reinforced electrostatic attractions between PFEBT$^-$ and BSA at low pH; likewise, increasing the pH from 7.4 to 14 induces and in turn strengthens electrostatic attractions between PFEBT$^+$ and lysozyme. With stronger electrostatic attractions, complexes are tightened for PFEBT$^-$/BSA and PFEBT$^+$/lysozyme, giving rise to enhanced polymer fluorescence and blue-shifted emission maxima. In addition, the large transformations in the PL maximum and intensity curves at pH close to the protein pIs

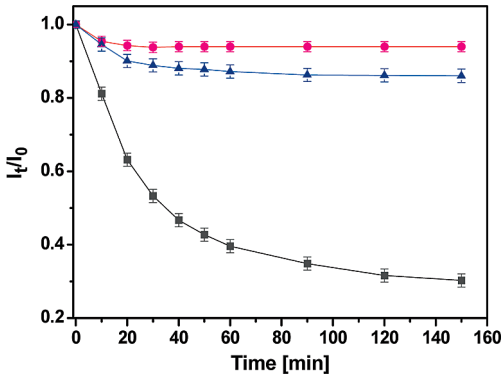

Figure 5. Relative PL intensities of PFEBT$^+$/BSA (circles), PFEBT$^-$/lysozyme (triangles), and PFEBT$^-$/BSA (squares) at 588 nm as a function of protein digestion time. [RU] = 6 μM and [protein] = 0.8 μM in 15 mM PBS at pH 7.4, excitation at 445 nm.

further support the proposed relationships between pH, electrostatic attractions, and the polymer fluorescence, as the net charge of proteins varies significantly around the pIs.

Fluorescence Variation upon Protein Digestion. The digestion process offers the possibility to study the effect of hydrophobic interaction on the polymer fluorescence, as the hydrophobic domains of protein can be demolished when protein is hydrolyzed into peptide segments.[27] In this consideration, BSA and lysozyme were digested by pepsin, and the fluorescence variation of PFEBT/protein complexes upon digestion was monitored. Pepsin is a protease that cleaves the peptide bonds on the amino side of Phe, Trp, or Tyr residues.[28] Noteworthy is that the presence of a small amount of pepsin in solution has no impact on the fluorescence of PFEBT$^-$ and PFEBT$^+$ at pH 7.4.

The relative PL intensities (I_t/I_0) at 588 nm for the polymer/protein complexes in 15 mM PBS at pH 7.4 as a function of digestion time are summarized in Figure 5. The polymer and protein concentrations are 6 and 0.8 μM, respectively. I_0 and I_t represent the PL intensities at 588 nm upon excitation at 445 nm before digestion and after digestion for t minutes, respectively. With the progress of digestion, the PL intensity decreases at a different rate for each polymer/protein pair. PFEBT$^-$/BSA has the largest intensity decrease rate among three polymer/protein pairs, which is followed by PFEBT$^-$/lysozyme and then PFEBT$^+$/BSA. At t = 150 min, the relative PL intensities do not change anymore, implying that further variation in the system resulting from digestion cannot be sensed by these polymers. In fact, according to the previous reports in which a similar digestion condition was used, the digestion of BSA and lysozyme is nearly completed at t = 150 min.[29] After proteins are digested for 150 min, the PL intensity decreases for PFEBT$^-$/BSA, PFEBT$^-$/lysozyme, and PFEBT$^+$/BSA are ~70, 14, and 6%, respectively.

Changes in electrostatic attractions and hydrophobic interactions are the origin of the difference in the fluorescence decrease of polymer/protein complexes upon digestion. Since BSA and lysozyme have net negative and positive charges at pH 7.4, respectively, electrostatic attractions are significant for PFEBT$^+$/BSA and PFEBT$^-$/lysozyme but neglectable for PFEBT$^-$/BSA. Electrostatic attractions hence play important roles in forming PFEBT$^+$/BSA and PFEBT$^-$/lysozyme complexes. Our previous report has shown that the strength of electrostatic attractions between CPE and biomolecules is mainly determined by the charge density of biomolecules.[30] Since the charge density of peptide fragments obtained from digestion is similar to that of the intact protein, electrostatic attractions within the intermolecular complexes cannot be significantly reduced by the digestion process. As a consequence, the fluorescence decreases after digestion for 150 min are not significant for oppositely charged PFEBT$^-$/lysozyme (~14%) and PFEBT$^+$/BSA (~6%). On the other hand, hydrophobic interaction is the main driving force for PFEBT$^-$/BSA complexation at pH 7.4. With the progress of digestion, BSA is gradually cleaved into charged fragments, and the surfactant nature of BSA is thus destroyed, leading to impaired hydrophobic interactions within the PFEBT$^-$/BSA system. Under these circumstances, most PFEBT$^-$ and the fragments cannot form tight complexes to induce effective polymer aggregation. As such, the fluorescence of PFEBT$^-$/BSA gradually decreases with the progress of digestion, and the fluorescence contrast before and after digestion for 150 min is prominent (~70%).

Conclusions and Summary Discussion

Cationic and anionic PFEBTs with an orange light-up signature toward proteins are designed and synthesized *via* Sonagashira condensation polymerization. The fluorescence of PFEBTs is dependent on the environmental polarity and is very weak in aqueous solution, owing to the charge transfer character of the excited states. Different from a majority of CPEs, PFEBTs exhibit fluorescence increase instead of self-quenching upon protein-induced polymer aggregation. PFEBTs thus resemble silole-based fluorophores with aggregation-induced emission (AIE) but differ in the operation mechanism, as AIE is derived from the constrained intramolecular rotation in the aggregated state.[31] In addition, the aggregation-enhanced fluorescence of PFEBTs is related to the complex structures that are governed by nonspecific interactions between the polymer and proteins. Such aggregation-mediated fluorescence turn-on behaviors of PFEBTs provide a straightforward channel to observe how electrostatic and hydrophobic interactions between CPEs and proteins influence the polymer fluorescence.

The general relationship between the polymer fluorescence and electrostatic attractions or hydrophobic interactions for PFEBTs/protein is illustrated in Scheme 2. For PFEBT/protein with the opposite charge sign (Scheme 2a), electrostatic attractions dominate PFEBT/protein complexation, giving rise to polymer aggregation and in turn enhanced polymer fluorescence. This is verified by the fluorescence increase for PFEBT$^+$ upon BSA addition (Figure 2b) as well as for PFEBT$^-$ upon lysozyme addition at pH 7.4 (Figure 3a). In addition, alternating the solution pH can inverse the net charges of proteins and thereby reinforce electrostatic attractions, leading to an increase in the polymer fluorescence (Figure 4). On the other hand, digestion cannot eliminate electrostatic attractions, and thereby the polymer fluorescence remains after digestion (Figure 5). For PFEBT/protein with the same charge sign (Scheme 2b), complexes can still form to generate a light-up signature for PFEBTs when hydrophobic interactions are remarkable. This happens to PFEBT$^-$/BSA rather than to PFEBT$^+$/lysozyme at pH 7.4 due to the surfactant nature of BSA (Figure 2a vs Figure 3b). In addition, the fluorescence of PFEBT$^-$/BSA is weaker than that of PFEBT$^+$/BSA at pH 7.4 (Figure 2c), implying the importance of additional electrostatic attractions in enhancing the polymer fluorescence. Since the hydrophobicity of protein is strongly dependent on its size and three-dimensional structure, it can be minimized by digestion. As such, the fluorescence for PFEBT^{-+}/BSA is turned off by the digestion process (Figure 5).

In conclusion, these findings illustrate the feasibility of exerting nonspecific interaction induced perturbation in the

SCHEME 2: Illustration of Fluorescence Responses of Cationic (a) and Anionic (b) Light-Up PFEBTs toward Protein and Its Fragments[a]

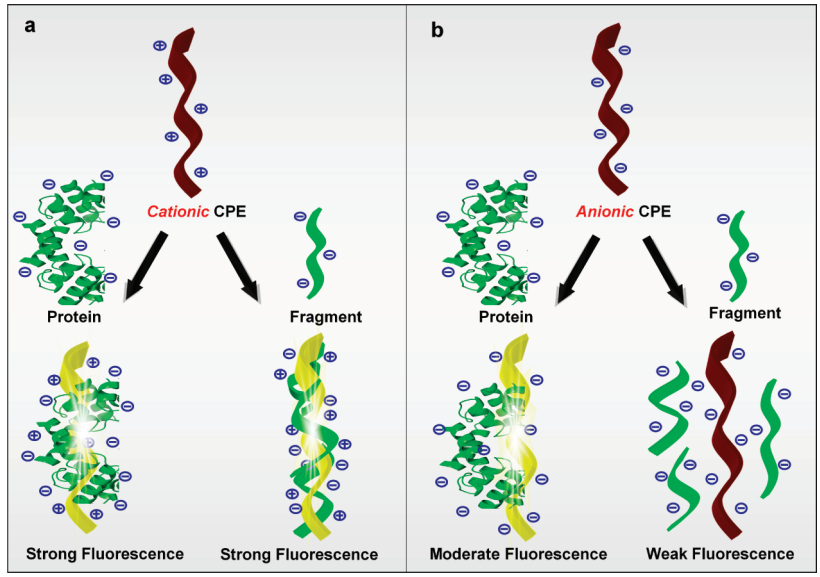

[a] The proteins and peptide fragments in parts a and b are the same.

optical feature of light-up CPEs to contrive label-free protein biosensors. For example, protein quantification could be performed on the basis of either electrostatic attraction or hydrophobic interaction induced light-up signature of PFEBTs. Moreover, hydrophobicity-dominated interactions between $PFEBT^-$/BSA complexes could be applied to monitor protease activity according to its light-off signature upon digestion. Apart from PFEBTs, other CPEs that can generate colorimetric or ratiometric signals toward proteins should also comply with these interacting patterns.

Experimental Section

Materials. 10× PBS buffer with pH 7.4 (ultrapure grade) is a commercial product of first BASE Singapore. Milli-Q water (18.2 MΩ) was used to prepare the buffer solutions from the 10× PBS stock buffer. 1× PBS contains NaCl (137 mM), KCl (2.7 mM), Na_2HPO_4 (10 mM), and KH_2PO_4 (1.8 mM). HCl (0.1 M) and NaOH (0.1 M) were used to adjust the pH of the PBS buffer solutions. Fresh stock solutions for $PFEBT^-$ (1 mM), $PFEBT^+$ (1 mM), BSA (1 mM), lysozyme (1 mM), and pepsin (1 mM) were prepared before use. A Millipore Millex syringe driven filter unit (0.22 μm, PVDF) was used to exclude the insoluble substances in the polymer solution before the dialysis process. Fisher brand regenerated cellulose dialysis tubing with a 3.5 kDa molecular weight cutoff was used for polymer dialysis. NMR solvents, D_3-chloroform (99%) and D_4-methanol (99.5%), were purchased from Cambridge Isotope Laboratories, Inc. 4,7-Dibromobenzothiadiazole and 2,7-dibromo-9,9-bis(6′-bromohexyl)fluorene were synthesized according to our previous report.[17] Other chemicals and biological reagents were purchased from Sigma-Aldrich Chemical Co., and were used as received.

Instruments. The NMR spectra were collected on a Bruker Avance 500 (DRX 500, 500 MHz). The mass spectra were obtained by using a Bruker Daltonics Autoflex II TOF system. Matrix-assisted laser desorption/ionization time-of-flight (MALDI-TOF) was performed by using 2,5-dihydroxybenzoic acid (DHB) as the matrix under the reflector mode for data acquisition. UV−vis spectra were recorded on a Shimadzu UV-1700 spectrometer. Fluorescence measurements were carried out on a Perkin-Elmer LS-55 equipped with a xenon lamp excitation source and a Hamamatsu (Japan) 928 PMT, using 90° angle detection for solution samples. Quantum yields were measured using quinine sulfate as the standard, with a quantum yield of 55% in H_2SO_4 (0.1 M). The solution pH was measured by a pH meter (Sartorius PB-10) with a glass/reference electrode calibrated with buffer solutions of pH 4, 7, and 10. Incubation experiments were conducted with eppendorf thermo mixer compact. Free drying was performed using Martin Christ Model Alpha 1-2/LD. All PL and UV measurements were carried out at 24 ± 1 °C.

Digestion Procedure. A solution of BSA or lysozyme (0.1 mM) and pepsin (0.01 mM) in 50 mM PBS buffer solution at pH 3 was incubated and shaken at 37 °C.[29] At intervals of 10 min, 20 μL of digestion solution was taken out and adjusted to pH 7.4 for PL measurement.

Synthesis of 4,7-Bis(2-(trimethylsilyl)ethynyl)benzothiadiazole (1). A solution of trimethylsilyl acetylene (1.08 g, 1.55 mL, 11.0 mmol, d = 0.695 g/mL) in $(i\text{Pr})_2\text{NH}$ (15.0 mL) was slowly added to a solution of 4,7-dibromobenzothiadiazole (1.47 g, 5.0 mmol), $Pd(PPh_3)_4$ (145 mg, 0.125 mmol), and CuI (47 mg, 0.25 mmol) in the mixture of $(i\text{Pr})_2\text{NH}$ (30 mL) and THF (10 mL) under nitrogen at room temperature. The reaction mixture was then stirred at 70 °C for 12 h. The solvent was removed under reduced pressure, and the residue was chromatographed on silica gel using dichloromethane/hexane (1: 4) as eluent to give **1** (2.5 g, 75%) as pale yellow crystals. ^{1}H NMR (500 MHz, CD_3Cl, δ ppm): 7.70 (s, 2 H), 0.33 (s, 18 H). ^{13}C NMR (125 MHz, CD_3Cl, δ ppm): 154.25, 133.14, 117.29, 103.65, 100.01, 0.11. MS (MALDI-TOF): m/z 328.07 $[M]^+$.

Synthesis of 4,7-Diethynylbenzothiadiazole (2). A mixture of methanol (10.0 mL) and NaOH solution (1.5 mL, 5 M) was slowly added to the solution of **1** (2 g, 6.0 mmol) in THF (20.0 mL) under nitrogen at 0 °C in dark. The reaction mixture was stirred for 3 h at 0 °C and then extracted with dichloromethane. The organic fraction was washed with water and dried over sodium sulfate, and the solvent was evaporated at 5 °C. The resulting brown residue was purified using silica gel chromatograph with dichloromethane/hexane (1: 2) as eluent to afford **2** (0.88 g, 80%) as yellow crystals. Compound **2** was stored in the dark under nitrogen at −10 °C before use. ^{1}H NMR (500

MHz, CD_3Cl, δ ppm): 7.36 (s, 2 H), 3.68 (s, 2 H). ^{13}C NMR (125 MHz, CD_3Cl, δ ppm): 154.18, 133.24, 116.78, 85.53, 78.91.

Synthesis of 2,7-Dibromo-9,9-bis(4′-sulfonatobutyl)fluorene disodium (3). 2,7-Dibromofluorene (4 g, 12 mmol) and tetrabutylammoium bromide (80 mg) were dissolved in the mixture of a 50 wt % aqueous solution of sodium hydroxide (8 mL) and dimethylsulfoxide (DMSO) (60 mL). A solution of 1,4-butane sultone (4 g, 29 mmol) in DMSO (20 mL) was added dropwise into the mixture under nitrogen. After stirring at room temperature for 4 h, the reaction mixture is precipitated into acetone to afford a crude product. The product was collected by filtration, washed with ethanol, recrystallized twice from acetone/H_2O, and dried under a vacuum at 60 °C for 24 h to yield **3** (4.3 g, 58.6%) as white needle crystals. ^1H NMR (500 MHz, CD_3OD, δ ppm): 7.68 (d, $J = 8.11$ Hz, 2 H), 7.63 (d, 2 H, $J = 1.45$ Hz), 7.52 (dd, 2 H, $J = 1.42$, 8.08 Hz), 2.68−2.47 (m, 4 H), 2.22−2.00 (m, 4 H), 1.62 (td, 4 H, $J = 7.83$, 7.83, and 15.65 Hz,), 0.67 (td, 4 H, $J = 7.83$, 7.83, and 15.65 Hz,). ^{13}C NMR (125 MHz, CD_3OD, δ ppm): 153.39, 140.68, 131.61, 127.38, 122.74, 122.52, 52.37, 40.76, 26.19, 24.25. MS (MALDI-TOF): m/z 619.89 $[M\text{-}Na]^-$.

Synthesis of 2,7-Dibromo-9,9-bis(6′-(*N*,*N*,*N*,-trimethylammonium)-hexyl)fluorene dibromide (4). Condensed trimethylamine (2 mL) was added dropwise to a solution of 2,7-dibromo-9,9-bis(6′-bromohexyl)fluorene (200 mg, 0.31 mmol) in THF (5 mL) at −78 °C. The mixture was allowed to warm to room temperature. The precipitate was redissolved by the addition of water (5 mL). After the mixture was cooled to −78 °C, additional trimethylamine (2 mL) was added. The mixture was stirred at room temperature for 24 h. After removal of the solvent, acetone was added to precipitate **4** (226 mg, 98%) as white powders. ^1H NMR (500 MHz, CD_3OD, δ ppm): 7.78 (d, 2 H, $J = 8.13$ Hz), 7.71 (d, 2 H, $J = 1.42$ Hz), 7.59 (dd, 2 H, $J = 1.62$ and 8.08 Hz), 3.38−3.31 (m, 4 H), 3.17 (s, 18 H), 2.22−2.07 (m, 4 H), 1.75−1.59 (m, 4 H), 1.34−1.17 (m, 8 H), 0.78−0.60 (m, 4 H). ^{13}C NMR (125 MHz, CD_3OD, δ ppm): 153.70, 140.71, 131.57, 127.38, 122.68, 122.68, 122.61, 67.66, 56.92, 53.57, 40.66, 29.95, 26.67, 24.48, 23.54. MS (MALDI-TOF): m/z 685.18 $[M\text{-}Br]^+$.

Synthesis of Poly[9,9-bis(4′-sulfonatobutyl)fluorenyleneethynylene-*alt*-4,7-(2,1,3,-benzothiadiazole) Disodium] (PFEBT$^-$). A two-necked flask was charged with **3** (160 mg, 0.25 mmol), **2** (46.8 mg, 0.26 mmol), $Pd(PPh_3)_4$ (14.5 mg, 1.25 μmol), and CuI (1.85 mg, 0.02 mmol). After degassing with one vacuum-nitrogen cycle, H_2O (1 mL), DMF (2 mL), and $(i\text{Pr})_2NH$ (1.5 mL) were added at −78 °C. The mixture was further frozen, evacuated, and thawed three times to further remove oxygen in the solvent. The polymerization was carried out at 70 °C under nitrogen in the dark for 24 h. The reaction mixture was cooled and then precipitated into acetone to yield the crude product as dark powders. It was redissolved in water, and treated with sodium sulfide (0.1 g). The solution was filtered through a 0.22 μm syringe driven filter to give limpid brown solution. Finally, the polymer was purified by dialysis against Mill-Q water using a 3.5 kDa molecular weight cutoff dialysis membrane for 5 days. After freeze-drying, PFEBT$^-$ (74 mg, 45%) was obtained as deep orange powders. ^1H NMR (500 MHz, CD_3OD, δ ppm): 8.03−7.31 (m, 8 H), 2.65−2.44 (m, 4 H), 2.26−1.97 (m, 4 H), 1.69−1.51 (m, 4 H), 0.87−0.47 (m, 4 H). ^{13}C NMR (125 MHz, CD_3OD, δ ppm): 155.40, 153.41, 140.69, 133.90, 133.71, 132.53, 132.34, 131.69, 128.37, 127.42, 122.75, 122.52, 99.15, 55.39, 52.42, 33.73, 26.21, 24.25.

Synthesis of Poly[9,9-bis(6′-(*N*,*N*,*N*,-trimethylammonium)-hexyl)fluorenyleneethynylene-*alt*-4,7-(2,1,3,-benzothiadiazole) Dibromide] (PFEBT$^+$). A two-necked flask was charged with **4** (157 mg, 0.25 mmol), **2** (46.8 mg, 0.26 mmol), $Pd(PPh_3)_4$ (14.5 mg, 1.25 μmol), and CuI (1.85 mg, 0.01 mmol). After degassing with one vacuum-nitrogen cycle, H_2O (1 mL), DMF (2 mL), and $(i\text{Pr})_2NH$ (1.5 mL) were added at −78 °C. The mixture was frozen, evacuated, and thawed three times to further remove oxygen in the solvent. The polymerization was carried out at 70 °C under nitrogen in the dark for 24 h. The reaction mixture was cooled and then precipitated into acetone to give the crude product as dark powders. The solution was filtered through a 0.22 μm syringe driven filter to give limpid brown solution. Finally, the polymer was purified by dialysis against Mill-Q water using a 3.5 kDa molecular weight cutoff dialysis membrane for 5 days. After freeze-drying, PFEBT$^+$ (95 mg, 48%) was obtained as deep orange powders. ^1H NMR (500 MHz, CD_3OD, δ ppm): 8.14−7.42 (m, 8 H), 3.30−3.19 (m, 4 H), 3.16−3.00 (m, 18 H), 2.45−1.94 (br, 4 H), 1.43−1.06 (br, 8 H), 0.89−0.45 (br, 4 H). ^{13}C NMR (125 MHz, CD_3OD, δ ppm): 155.68, 152.54, 143.01, 134.25, 133.59, 133.92, 133.22, 132.57, 127.98, 127.42, 123.52, 121.58, 98.90, 98.00, 67.78, 56.67, 53.59, 40.79, 31.03, 26.73, 24.58, 23.63.

Acknowledgment. The authors are grateful to the National University of Singapore (YIA R-279-000-234-123), and Singapore Ministry of Education (R-279-000-255-112) for financial support.

References and Notes

(1) (a) Dubertret, B.; Calame, M.; Libchaber, A. *Nat. Biotechnol.* **2001**, *19*, 365–370. (b) Bunka, D. H. J.; Stockley, P. G. *Nat. Rev. Microbiol.* **2006**, *4*, 588–596. (c) Sassolas, A.; Leca-Bouvier, B. D.; Blum, L. J. *Chem. Rev.* **2008**, *108*, 109–139.

(2) Kodadek, T. *Chem. Biol.* **2001**, *8*, 105–115.

(3) Wright, A. T.; Anslyn, E. V. *Chem. Soc. Rev.* **2006**, *35*, 14–28.

(4) (a) Thomas, S. W., III; Joly, G. D.; Swager, T. M. *Chem. Rev.* **2007**, *107*, 1339–1380. (b) Herland, A.; Inganäs, O. *Macromol. Rapid Commun.* **2007**, *28*, 1703–1713. (c) Nilsson, K. P. R.; Hammarström, P. *Adv. Mater.* **2008**, *20*, 2639–2645.

(5) (a) Swager, T. M. *Acc. Chem. Res.* **1998**, *31*, 201–207. (b) McQuade, D. T.; Pullen, A. E.; Swager, T. M. *Chem. Rev.* **2000**, *100*, 2537–2574. (c) Pu, K. Y.; Liu, B. *Biosens. Bioelectron.* **2009**, *24*, 1067–1073.

(6) (a) Chen, L.; McBranch, D. W.; Wang, H. L.; Helgeson, R.; Wudl, F.; Whitten, D. G. *Proc. Natl. Acad. Sci. U.S.A.* **1999**, *96*, 12287–12292. (b) Wang, D.; Gong, X.; Heeger, P. S.; Rininsland, F.; Bazan, G. C.; Heeger, A. J. *Proc. Natl. Acad. Sci. U.S.A.* **2002**, *109*, 49–53. (c) Ho, H. A.; Leclerc, M. *J. Am. Chem. Soc.* **2004**, *126*, 1384–1387. (d) Ho, H. A.; Najari, A.; Leclerc, M. *Acc. Chem. Res.* **2008**, *41*, 168–178.

(7) Wang, J.; Liu, B. *Chem. Commun.* **2009**, 2284–2286.

(8) (a) Heeger, P. S.; Heeger, A. J. *Proc. Natl. Acad. Sci. U.S.A.* **1999**, *96*, 12219–12221. (b) Dwight, S. J.; Gaylord, B. S.; Hong, J. W.; Bazan, G. C. *J. Am. Chem. Soc.* **2004**, *126*, 16850–16859.

(9) (a) Fan, C.; Plaxco, K. W.; Heeger, A. J. *J. Am. Chem. Soc.* **2002**, *124*, 5642–5643. (b) Kim, I.-B.; Dunkhorst, A.; Bunz, U. H. F. *Langmuir* **2005**, *21*, 7985–7989. (c) You, C. C.; Miranda, O. R.; Gider, B.; Ghosh, P. S.; Kim, I. B.; Erdogan, B.; Krovi, S. A.; Bunz, U. H. F.; Rotello, V. M. *Nat. Nanotechnol.* **2007**, *2*, 318–323. (d) Zhang, Y.; Liu, B.; Cao, Y. *Chem. Asian J.* **2008**, *3*, 739–745.

(10) Miranda, O. R.; You, C. C.; Phillips, R.; Kim, I. B.; Ghosh, P. S.; Bunz, U. H. F.; Rotello, V. M. *J. Am. Chem. Soc.* **2007**, *129*, 9856–9857.

(11) (a) Yu, D.; Zhang, Y.; Liu, B. *Macromolecules* **2008**, *41*, 4003–4011. (b) Pu, K. Y.; Zhan, R.; Liu, B. *Chem. Commun.* **2010**, DOI: 10.1039/b915984c.

(12) (a) Ho, H. A.; Boissinot, M.; Bergeron, M. G.; Corbeil, G.; Doré, K.; Boudreau, D.; Leclerc, M. *Angew. Chem., Int. Ed.* **2002**, *41*, 1548–1551. (b) Li, C.; Numata, M.; Takeuchi, M.; Shinkai, S. *Angew. Chem., Int. Ed.* **2005**, *44*, 6371–6374. (c) Pu, K. Y.; Pan, S. Y. H.; Liu, B. *J. Phys. Chem. B* **2008**, *112*, 9295–9300.

(13) (a) Burrows, H. D.; Lobo, V. M. M.; Pina, J.; Ramos, M. L.; Seixas de Melo, J.; Valente, A. J. M.; Tapia, M. J.; Pradhan, S.; Scherf, U. *Macromolecules* **2004**, *37*, 7425–7427. (b) Li, C.; Numata, M.; Bae, A. H.; Sakurai, K.; Shinkai, S. *J. Am. Chem. Soc.* **2005**, *127*, 4548–4549. (c) Al Attar, H. A.; Monkman, A. P. *J. Phys. Chem. B* **2007**, *111*, 12418–12426.

(14) (a) Liu, B.; Bazan, G. C. *J. Am. Chem. Soc.* **2004**, *126*, 1942–1943. (b) Hong, J. W.; Hemme, W. L.; Keller, G. E.; Rinke, M. T.; Bazan, G. C. *Adv. Mater.* **2006**, *18*, 878–882. (c) Chi, C.; Mikhailovsky, A.; Bazan, G. C. *J. Am. Chem. Soc.* **2007**, *129*, 11134–11145.

(15) Pu, K. Y.; Liu, B. *Macromolecules* **2008**, *41*, 6636–6640.

(16) (a) Pu, K. Y.; Liu, B. *Adv. Funct. Mater.* **2009**, *19*, 277–284. (b) Pu, K. Y.; Cai, L.; Liu, B. *Macromolecules* **2009**, *42*, 5933–5840.

(17) Liu, B.; Bazan, G. C. *Nat. Protoc.* **2006**, *1*, 1698–1702.

(18) (a) Pu, K. Y.; Qi, X. Y.; Yang, Y. L.; Lu, X. M.; Li, T. C.; Fan, Q. L.; Wang, C.; Liu, B.; Chan, H. S. O.; Huang, W. *Chem.—Eur. J.* **2008**, *14*, 1205–1215. (b) Pu, K. Y.; Zhang, B.; Ma, Z.; Wang, P.; Qi, X. Y.; Chen, R. F.; Wang, L. H.; Fang, Q. L.; Huang, W. *Polymer* **2006**, *47*, 1970–1978.

(19) Kato, S. I.; Matsumoto, T.; Shigeiwa, M.; Gorohmaru, H.; Maeda, S.; Ishi-i, T.; Mataka, S. *Chem.—Eur. J.* **2006**, *12*, 2303–2317.

(20) Huang, F.; Wang, X.; Wang, D.; Yang, W.; Cao, Y. *Polymer* **2005**, *46*, 12010–12015.

(21) (a) Cornil, J.; Gueli, I.; Dkhissi, A.; Sancho-Garcia, J. C.; Hennebicq, E.; Calbert, J. P.; Lemaur, V.; Beljonne, D.; Brédas, J. L. *J. Chem. Phys.* **2003**, *118*, 6615–6623. (b) Fratiloiu, S.; Fonseca, S. M.; Grozema, F. C.; Burrows, H. D.; Costa, M. L.; Charas, A.; Morgado, J.; Siebbeles, L. D. A. *J. Phys. Chem. C* **2007**, *111*, 5812–5820.

(22) (a) Tong, H.; Hong, Y.; Dong, Y.; Häu*β*ler, M.; Lam, J. W. Y.; Li, Z.; Guo, Z.; Guo, Z.; Tang, B. Z. *Chem. Commun.* **2006**, 3705–3707. (b) Tong, H.; Hong, Y.; Dong, Y.; Häussler, M.; Li, Z.; Lam, J. W. Y.; Dong, Y.; Sung, H. H. Y.; Williams, I. D.; Tang, B. Z. *J. Phys. Chem. B* **2007**, *111*, 11817–11823.

(23) Nelson, D. L.; Cox, M. M. *Lehninger Principles of Biochemistry*, 4th ed.; W. H. Freeman: New York, 2004.

(24) Peters, T. J. *Adv. Protein Chem.* **1985**, *37*, 161–245.

(25) Shi, Q.; Zhou, Y.; Sun, Y. *Biotechnol. Prog.* **2005**, *21*, 516–523.

(26) Yang, A. S.; Honig, B. *J. Mol. Biol.* **1993**, *231*, 459–474.

(27) (a) He, X. M.; Carter, D. C. *Nature* **1992**, *358*, 209–215. (b) Petitpas, I.; Bhattacharya, A. A.; Twine, S.; East, M.; Curry, S. *J. Biol. Chem.* **2001**, *276*, 22804–22809.

(28) Fruton, J. S. *Q. Rev. Biol.* **2002**, *77*, 127–147.

(29) (a) Joy, H. K.; Te, P. K. *J. Biol. Chem.* **1977**, *252*, 4326–4329. (b) Thilo, F. A.; Jürgen, K.; Bruns, K.; Michael, P. *J. Am. Soc. Mass Spectrom.* **1999**, *10*, 112–118.

(30) Pu, K. Y.; Fang, Z.; Liu, B. *Adv. Funct. Mater.* **2008**, *18*, 1321–1328.

(31) (a) Chen, J. W.; Law, C. C. W.; Lam, J. W. Y.; Dong, Y. P.; Lo, S. M. F.; Williams, I. D.; Zhu, D. B.; Tang, B. Z. *Chem. Mater.* **2003**, *15*, 1535–1546. (b) Chen, J.; Peng, H.; Law, C. C. W.; Dong, Y.; Lam, J. W. Y.; Williams, I. D.; Tang, B. Z. *Macromolecules* **2003**, *36*, 4319–4327.

JP906433U